Adipose-derived Stem Cells Induced EMT-like Changes in H358 Lung Cancer Cells

YOUNG MIN PARK[1,2], SUNG HONG YOO[2] and SUNG-HYUN KIM[1]

[1]DMC BioMedical Research Center and [2]DMC Hepatology Center, Bundang Jesaeng General Hospital, Seongnam, Republic of Korea

Abstract. *Despite the potential utility of adipose-derived mesenchymal stem cells (ADSCs) in regenerative medicine, not much is known about their interaction with residual cancer cells. Here, we studied the direct co-culture effects of ADSCs on H358 lung cancer cells. The paracrine effects of ADSCs were compared to those of the cancer-associated fibroblasts. Extracellular matrix and conditioned media were used to determine the underlying molecules. Time-lapse photography, fluorescence-activated cell sorting (FACS), scratch assays, immunocytochemistry, and reverse-transcription polymerase chain reaction were used to analyze the effects. ADSCs differentiated into myofibroblasts expressing αSMA, and H358 cells strongly attached to them. EMT-like changes were observed in H358 cells which were inhibited by γ-secretase inhibitor, a-NOTCH inhibitor. Surprisingly, both mesenchymal and epithelial genes were expressed, and the effects were readily reversed when cells were sorted by FACS. These data suggest that ADSCs may differentiate into tumor stroma that plays supportive roles during cancer progression.*

Malignant progression is driven by cell autonomous genetic alterations in cancer cells, and selected by the non-cell autonomous effects of the tumor microenvironment (1-3). Cancer-associated fibroblasts (CAFs) are the most abundant stromal cellular components that are known to nest and nurture the cancer cells (4-6). Recently cell therapies using adipose-derived mesenchymal stem cells (ADSCs) have been frequently employed to treat various aging-related degenerative diseases or for reconstruction after oncological surgery (7, 8). In contrast to accumulating data on their multipotency to differentiate into various normal tissues, little has been reported about their unintended interaction with cancer cells, which seemed to promote cancer cell proliferation or metastasis in endometrial, stomach, and breast cancer (9-11). In the present study, we examined the direct interaction between ADSCs and H358 lung cancer cells *in vitro*. It is noteworthy that closely-related to ADSCs, bone marrow-derived mesenchymal stem cells (MSCs) are intimately associated with cirrhosis, fibrosis, and malignant transformation; they are attracted to the inflammatory signals released from tumors, infiltrated, and differentiated into CAFs that are marked by the aberrant expression of alpha-smooth muscle actin (αSMA) (12, 13). Although there is little evidence that ADSCs increase the risk of cancer (14), they seem to have full potential to differentiate into stromal myofibroblasts that play a deterministic role in tumor characteristics, such as growth, metastasis, and drug resistance (15-18), which may help recapitulate the tumor microenvironments *in vitro* (19).

CAFs have been shown to promote epithelial- mesenchymal transition (EMT) in cancer cells (20-23). EMT renders cancer cells migratory and resistant to epithelial-targeted drugs as the cellular mechanism driving malignant progression (24-27). Cellular hallmarks of EMT include loss of E-cadherin-mediated homotypic cell adhesion, the loss of lamellipodia, and the gain of elongated fusiform filopodia (28). *In vivo*, EMT is frequently observed in the invasive front where malignant cancer cells are detached and migrate away from the tumor nodules (29, 30). Various ligands released by CAFs have been reported to induce EMT in cancer cells, including transforming growth factor-β1 (TGFβ1) (31, 32), WNT (30, 33), JAGGED, NOTCH (34), hepatocyte growth factor (HGF) (35), collagen I (COLI) (36), or oxidative stress (37). During EMT, NOTCH and TGFb signaling converge to SMAD3 pathway (38, 39). TWIST, Snail1 (SNAI1), and zinc finger E-box-binding hemeobox 1, 2 (*ZEB1, 2*) are up-regulated, which represses E-cadherin (CDH1) expression (40). In prostate cancer, CAFs were shown to induce EMT by engaging in Warburg metabolism that generates oxidative stress (41). In response, hypoxia-induced factor-1α (HIF1α) was activated in cancer

Correspondence to: Sung-Hyun Kim, Ph.D., DMC BioMedical Research Center, Bundang Jesaeng General Hospital, 255-2 Seohyun Ro 180 Gil, Bundang Gu, Seongnam Si, Kyungki-do 463-774, Korea. Tel: +82 1090975365, e-mail: genpax@daum.net

Key Words: ADSC, EMT, H358 cells, tumor microenvironment, cancer-associated fibroblasts, αSMA.

cells, which up-regulated SNAI1 expression (41). Furthermore, recent studies showed MSC-derived myofibroblasts induced EMT in pancreatic cancer cells *via* the JAGGED-NOTCH pathway (13).

In this study, we analyzed the paracrine effects of ADSCs on H358 lung cancer cells.

Materials and Methods

Cell culture. Human ADSCs were purchased from Cambrex (Lonza Walkersville, MD, USA), and cultured in ADSC growth medium: Minimum essential mediaum (MEM) alpha (Gibco, Gaithersburg, MD, USA) supplemented with 10% fetal bovine serum (FBS) (Hyclone, Logan, UT, USA), 100 mM sodium pyruvate (Gibco), and 100 units of penicillin/100 μg/ml streptomycin (Gibco). Upon 80~90% confluence, ADSCs were maintained in differentiation media with low serum, 1% FBS, supplemented with TGF-β, 7.5 ng/ml (13), and 400 μg/ml heparin for three days. Human lung cancer H358 cells were obtained from the Korea Cell Line Bank (Seoul, Korea) and transfected with green fluorescent protein (GFP) construct as previously described (39), and cultured in cancer growth medium: RPMI1640 (Gibco) supplemented with 10% FBS, 100 units of penicillin/100 μg/ml streptomycin (Gibco). Cells were cultured at 37˚C, with 5% CO_2, and all assays were carried out with MSCs and CAFs of passage six or less.

Direct and indirect co-culture. To prepare conditioned media, ADSCs were cultured in the cancer growth medium for two days. The medium was centrifuged, and the top medium was taken gently without disturbing the pellet of cell debris. The conditioned media was frozen at –70˚C until use. About 20 lots of conditioned media were pooled together before use. The conditioned media were replaced every 24 h. For direct co-cultures, ADSCs were cultured in growth medium until 90%, and switched to the differentiation medium. After maintenance for three days, H358 cells were seeded directly on top, or on extracellular matrix (ECM) that was prepared by stepwise methanol treatment of 50%, 95%, 100%, followed by rehydration into the cancer growth medium. GFP-tagged lung cancer cells (2×10^3) were seeded either in the conditioned media, on ECM, or directly on top of live ADSCs. The number of cells and morphology of GFP-positive H358 cells were recorded daily under a fluorescence microscope (Zeiss, Oberkochen, Germany).

Attachment assay. FBS is enriched with a number of growth factors including fibroblast growth factors (FGFs) and transforming growth factors (TGFs) that render epithelial H358 cells fibrotic and more adhesive to culture dishes. To avoid this effect, defined ACL4 medium for lung cancer cells was used; RPMI 1640, supplemented with 0.02 mg/ml insulin, 0.01 mg/ml transferrin, 25 nM sodium selenite, 50 nM hydrocortisone, 1 ng/ml epidermal growth factor, 0.01 mM ethanolamine, 0.01 mM phosphorylethanolamine, 100 pM triodothyronine, 0.5% bovine serum albumin (BSA), 10 mM HEPES, 0.5 mM sodium pyruvate, and 2 mM L-glutamine. GFP-tagged H358 lung cancer cells (2×10^3) were seeded on 6-well plates: with live ADSCs, or ECM, or no treatment. After 24 hours of incubation, unattached H358 cells were gently washed away three times with PBS, and the remaining GFP-positive cells were counted under a fluorescence microscope.

Time-lapse photography and fluorescence-activated cell sorting. To determine the growth rates and cell motility, time-lapse photography was performed following the cells in the same positions of the culture dishes for 2-3 days. To show both the GFP-positive H358 cells and the negative ADSCs, photos were taken with both regular light and fluorescent light. To align the dishes in the same position, the bottoms of culture dishes were pre-marked with permanent markers, and photos were taken aligning the markers at the same positions every day. In multicellular colonies, particularly in multilayers of mesenchymal cells, individual cells were often indistinguishable. In those cases, to precisely score the cell numbers, cells were trypsinized, resuspended as single cells, and counted by FACSAriaIII (Becton Dickinson Biosciences, San Jose, CA, USA) using 488 nm optical filter.

Wound healing assay for cell motility. To test the effects of ADSCs on the motility of H358 cells, scratches were made with pipette tips, and how quickly the scratches were filled by neighboring cells was observed in the next 3-4 days. Approximately 1×10^4 GFP-tagged H358 cells were seeded on ADSCs, ECM, or no treatment as described for co-cultures. After 24 h of incubation, scratches were made with pipette tips and rulers. The scraped cells were removed, and the remaining cells were incubated for two more days. The GFP-positive H358 cells migrating into the scratched area were photographed and/or scored. All assays were performed in triplicate.

Immunocytochemistry. Immunocytochemistry was performed as described elsewhere (39). Briefly, cells were fixed with 4% paraformaldehyde for 10 min and permeablized with 0.5% Triton-X for 5 min, blocked with 1% BSA in PBS for one hour, and incubated with primary antibodies for two hours at room temperature, and incubated with secondary Alexa 594-conjugated anti-mouse IgF from Invitrogen (Carlsbad, CA, USA) for one hour. Additional reagents were purchased from Sigma Aldrich (St. Louis, MO, USA). The cells were washed with PBS, and were stained with 4',6-diamidino-2-phenylindole (DAPI) for nuclei as a counter staining (40). The cells were observed with a ZEISS FL Axiovert 200 Microscope (Zeiss, Oberkochen, Germany).

Quantitative reverse transcription polymerase chain reaction (RT-PCR). To compare gene expression levels quantitatively, total RNA was extracted from each cell type after sorting by FACSAriaIII (Becton Dickinson Biosciences) using 488 nm optical filter, or passaging after ADSCs were differentiated. cDNA was synthesized using oligo-dT primers and M-MLV reserse transcriptase (Invitrogen). Quantitative real-time RT-PCR was performed using Applied Biosystems 7900HT fast real-time PCR systems (Foster City, CA, USA), SYBR Green PCR master mix (Applied Biosystems), as described elsewhere (39). The following primers were used for each gene: *SNAI1*, F: 5'-CCTCCCTGTCAGATG AGGAC-3', R: 5'-CCAGGCTGAGGTATTCCTTG-3', *TWIST1*, F: 5'-GGAGTCCGCAGTCTTACGAG-3', R: 5'-TCTGGAGGACC TGGTAGAGG-3', *E-cadherin* (*CDH1*), F: 5'-TGCCCAGAAAAT GAAAAAGG-3', R: 5'-GTGTATGTGGCAATGCGTTC-3', *N-cadherin* (*CDH2*), F: 5'-ACAGTGGCCACCTACAAAGG-3', R: 5'-CCGAGATGGGGTTGATAATG-3', *Cytokeratin 19* (*CK19*), F: 5'-CCCGCGACTACAGCCACTA-3', R: 5'-GCTCATGCGCAGAG CCT-3', *Vimentin* (*VIM*), F: 5'-GAGAACTTTGCCGTTGAAGC-3', R: 5'-GCTTCCTGTAGGTGGCAATC-3', *fibroblast activation protein* (*FAP*), F: 5'-TCAACTGTGATGGCAAGAGCA-3', R: 5'-

TAGGAAGTGGGTCATGTGGGT-3', *α-SMA*, F: 5'-AGGGGGTG ATGGTGGGAATG-3', R: 5'-GCCCATCAGGCAACTCGTAAC-3', and *glyceraldehydes 3-phosphate dehydrogenase* (*GAPDH*), F: 5'-TGGACTCCACGACGTACTCAG-3', R: 5'-ACATGTTCCAATAT GATTCCA-3'. *GAPDH* was used as the house keeping gene for loading control. Relative expression levels were analyzed by the ΔΔCt method.

NOTCH inhibition. To determine the effects of NOTCH inhibition, a direct co-culture was established as described above, and γ-secretase inhibitor (GSI, Santa Cruz Biotech. Inc.), a potent NOTCH inhibitor, was added to the medium. GSI was dissolved in DMSO at 1 μM, and diluted 1000-fold to 1 nM in the culture media. The changes in cell morphology and motility of H358 cells were monitored by time-lapse photography for the next 24 h.

Results

H358 lung cancer cells attached to ADSC-derived myofibroblasts. To evaluate the potential of ADSCs to differentiate into tumor stroma, ADSCs were co-cultured with H358 lung cancer cells and the gene expression was examined (Figure 1A). Seeded on ADSCs, H358 cells were distinguished by stable GFP expression (Figure 1B). Within 6-24 h of co-culture, significantly more H358 cells were attached compared with monoculture condition. This was most dramatic in ACL4 medium, a defined medium for lung cancer cells, improving attachment approximately 20-fold or more (Figure 1C). When the medium was supplemented with 10% FBS, the effect was reduced to approximately 1.5-2.0-fold (Figure 1E). In monoculture conditions, high serum induced slightly fibrotic morphology with reduced homotypic adhesion and increased attachment to the culture dish. To test whether the attachment was enhanced by the secreted factors or the ECM laid by ADSCs, the effects of de-cellularized ECM were compared with those of conditioned media. The ECM of ADSCs reproduced the enhanced attachment (Figure 1C), but the conditioned media did not. To test whether they differentiated into stromal myofibroblasts, gene expression was examined by immunocytochemistry and by RT-PCR (Figure 2). Compared with normal skin fibroblasts (39) that did not induce *aSMA* expression (Figure 2A), ADSCs expressed *aSMA* and *CDH2* in similar levels to those of the CAFs and induced *aSMA* expression in H358 cells (Figure 2B, arrowheads). RT-PCR of the sorted cells also showed up-regulation of *aSMA* expression. *Sox2* expression was significantly reduced, indicating that terminal differentiation occurred (Figure 2D). These data indicate that ADSCs differentiated into stromal myofibroblasts that produce ECM that H358 lung cancer cells readily attached to.

ADSCs promoted the motility of H358 cells. In a recent report, primary CAFs promoted the motility of H358 cells (39). To see if ADSCs also stimulate the motility of H358 cells, time-lapse photography was used. When co-cultured with ADSCs, H358 cells became highly migratory, For example, they lost the homotypic adhesion that maintains the integrity of static epithelial colonies, and became fibrotic individual cells that moved around (Figure 3A). Neither ECM nor conditioned media could reproduce the morphological changes caused by direct contact of H358 cells with live ADSCs. To demonstrate the changes in cell motility, scratch assays were performed. Within 48 h after scratches were made, both ADSCs and H358 cells actively migrated into the scratched area (Figure 3B), but not in co-cultures with ECM or conditioned media where the gaps between colonies were slowly filled by static cell proliferation (Figure 3C and D). To test whether the co-culture effects were reversible, H358 cells were sorted from ADSCs by FACS for their GFP expression, and plated alone under a monoculture condition. H358 cells immediately regained their original non-migratory epithelial characteristics, indicating that the direct cell-cell contact with ADSC rendered them motile and fibrotic in a reversible manner.

EMT-like gene expression was induced in H358 cells. To examine the changes in gene expression associated with EMT in H358 cells, RT-PCR and immunocytochemistry were performed (Figure 4). *TWIST* and *SNAI1*, the transcription factors with potent EMT inducing activities, were significantly up-regulated, and consequently the downstream mesenchymal markers *CDH2* and *VIM* were also up-regulated. However, expression of epithelial markers, *CK19* and *CDH1*, was maintained at elevated levels (Figure 4C), indicating that the biphasic epithelial and mesenchymal state was induced. Compared with indirect co-cultures with the conditioned media and ECM, live ADSCs activated the expression of *TWIST, SNAI1, VIM* and *CDH2* in significantly higher levels. A similar EMT-like phenomenon was also observed when H358 cells were co-cultured with the primary CAFs, as shown in Figure 4F and G (unpublished data; 38). These gene expression data suggest that the EMT-like phenomenon in H358 cells, induced similarly by ADSCs and CAFs, is different from normal EMT in its transient, reversible, and biphasic nature.

Discussion

Despite the recent enthusiasm for cell therapies with ADSCs, not much is known about their unintended interaction with residual cancer cells. In this study, we co-cultured ADSCs with H358 lung cancer cells allowing for direct cell-cell interaction and found that ADSCs promoted the attachment of the cancer cells and induced an EMT-like phenomenon (Summarized in Figure 5A). As a lineage tracer for the cancer cells, stable GFP expression was used to score for changes in the number of cells and the cellular hallmarks of EMT: Loss-of homotypic cell adhesion of epithelial colonies,

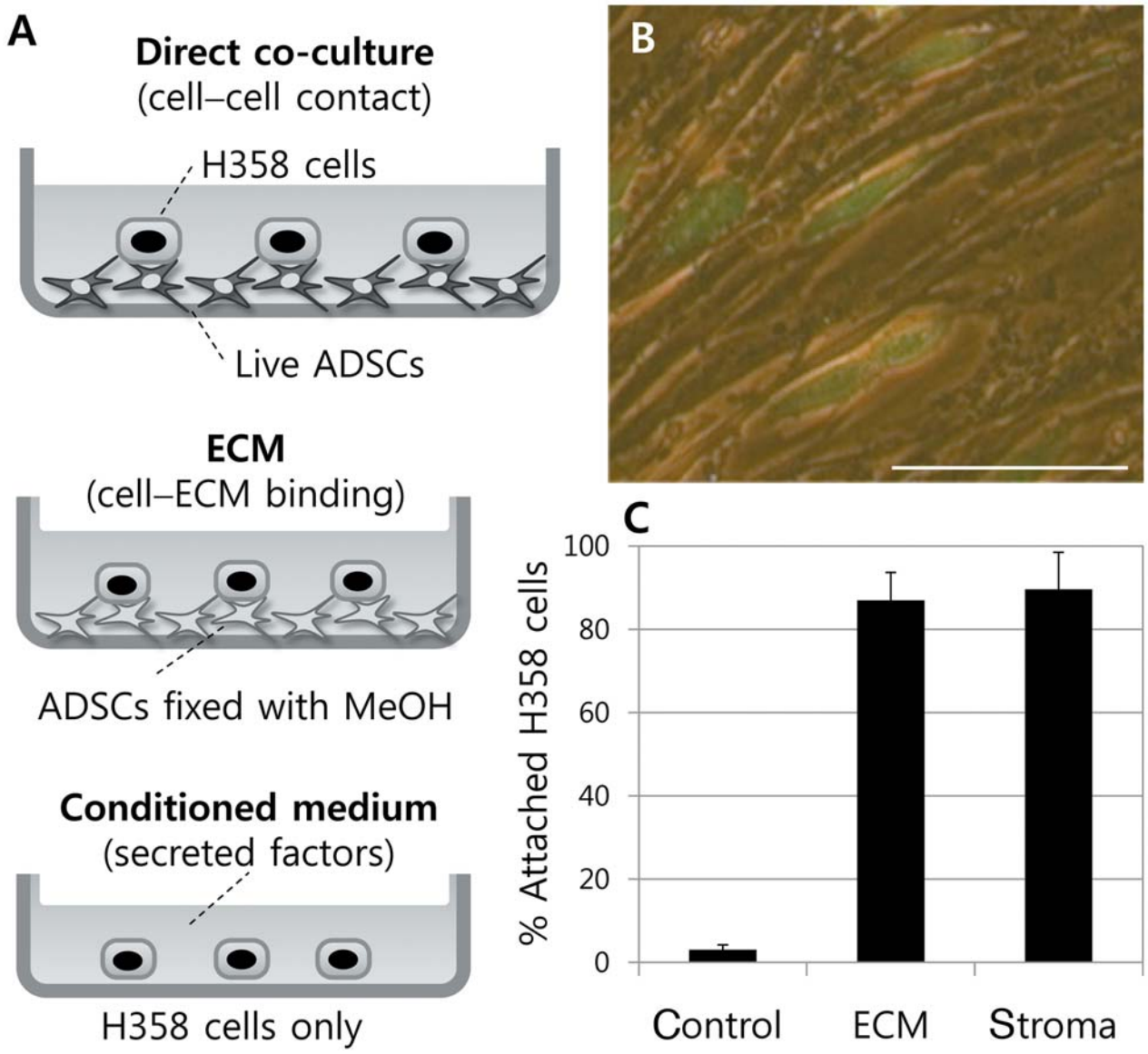

Figure 1. *H358 lung cancer cells strongly attached to extracellular matrix (ECM) of adpose-derived mesenchymal stem cells (ADSCs). Reaching 80-90% confluence in growth media, ADSCs were differentiated for three days supplemented with transforming growth factor-β1 (TGFβ1) in low serum. After direct co-culture with H358 lung cancer cells, or indirect with the ECM or conditioned media, gene expression was examined. A: Schematic drawing of co-cultures; H358 cells tagged with green fluorescent protein (GFP) were seeded on top of live ADSCs, after methanol treatment, or in conditioned media. B: GFP-positive (H358) and GFP-negative (ADSC) cells in co-culture were observed under fluorescence microscopy. Normal light was also used to show GFP-negative CAFs. Scale bar: 50 μm. C: Graphs showing the percentage of attached H358 cells in ACL4 medium. Control was H358 cells only; ECM was H358 cells seeded on ECM; stroma was H358 cells co-cultured with live ADSCs.*

gain-of fibrotic morphology with elongated filopodia, and gain of increased cell motility. Indirect co-cultures with the ECM promoted attachment, but not the EMT-like phenomenon, uncoupling the ECM-induced attachment from the EMT-like phenomenon. On the other hand, conditioned media did not reproduce the EMT-like phenomenon, suggesting that direct cell-cell signaling might be underlying it. To interfere with the NOTCH-mediated direct cell-cell communication, γ–secretase inhibitor was added to the media (1nM) on day 2 of co-culture. The EMT-like phenomenon was reversed; most of the mesenchymal cells disappeared and epithelial colonies started to appear within 24 h (Figure 5B). A spot in the culture marked by an asterisk shows the same position of the culture dish with

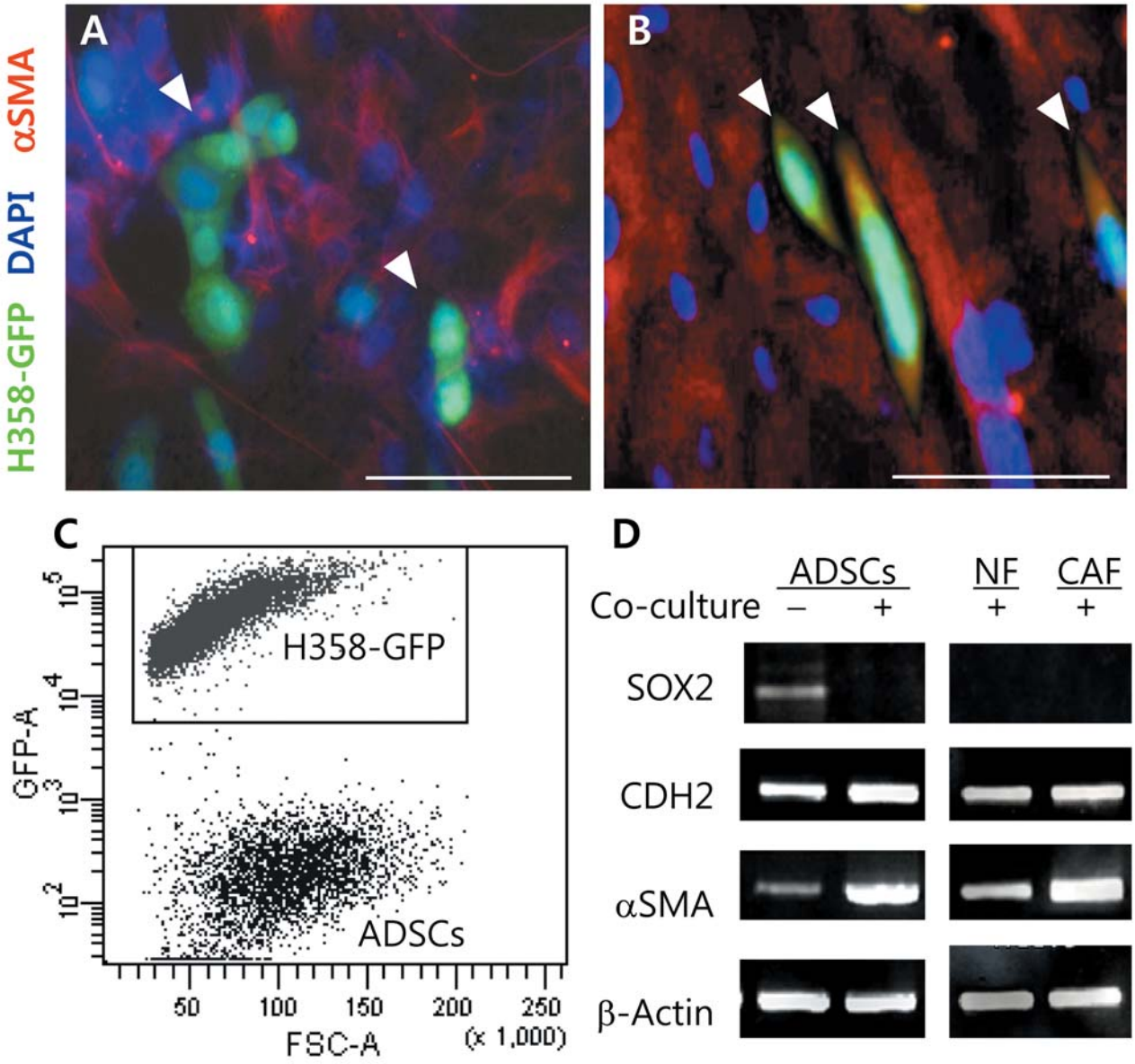

Figure 2. *Adpose-derived mesenchymal stem cells (ADSCs) differentiated into myofibroblasts when co-cultured with H358 lung cancer cells. Gene expression underlying myofibroblast differentiation was examined by immunocytochemistry and RT-PCR. GFP-posive H358 cells and GFP-negative ADSCs were stained red for αSMA and counterstained with 4',6-diamidino-2-phenylindole (DAPI; blue). A: When co-cultured with normal fibroblasts, H358 cells exhibited epithelial characteristics and low αSMA expression. B: When co-cultured with ADSCs αSMA expression was up-regulated in both ADSCs and H358 cells (white arrowheads), Scale bar: 50 μm. C: To quantitatively determine the gene expression levels, ADSCs and H358 cells were sorted by FACS after two days of co-culture. D: RT-PCR of SOX2, CDH1, CDH2 and aSMA, showing differentiation of ADSCs into myofibroblasts.*

mesenchymal GFP-positive cells migrated around dynamically. These results suggest that ADSCs may attach to cancer cells and induce EMT-like changes in H358 cells.

At the gene expression level, ADSCs were reminiscent of the primary CAFs. Particularly, αSMA expression was up-regulated at similar levels, indicating that ADSCs differentiated into myofibroblasts. ADSCs are multipotent adult stem cells that can differentiate into various tissue types depending on the cellular context, and our data suggest that H358 lung cancer cells triggered differentiation into the myofibroblast lineage. MSCs, closely related adult stem cells of mesodermal origin, were recently shown to differentiate into CAFs and induce EMT in pancreatic cancer cells through the NOTCH pathway (13). Diversity of tumor

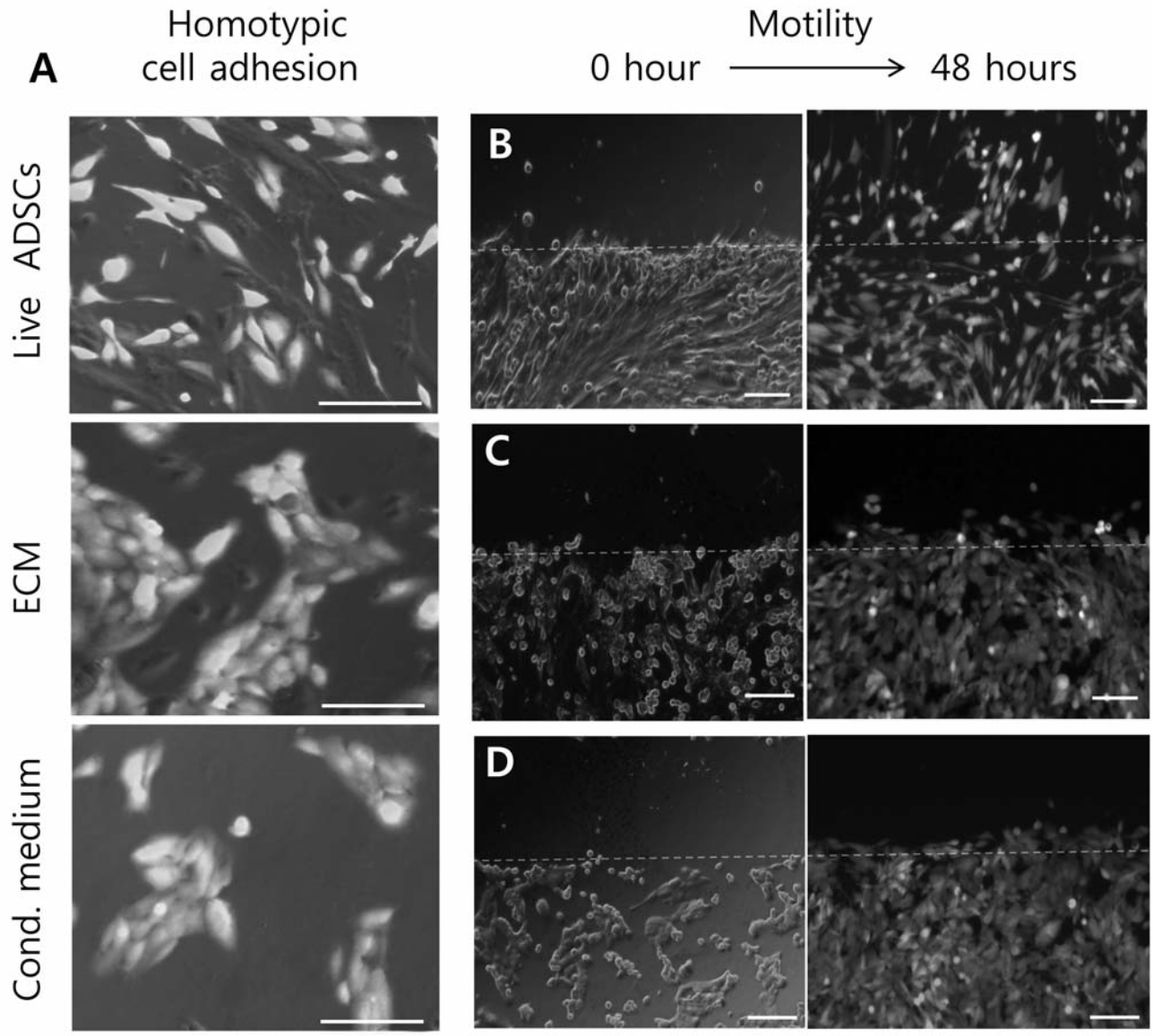

Figure 3. *Adipose-derived mesenchymal stem cells (ADSCs) increased motility of H358 cells. Co-cultured with ADSCs, H358 cells exhibited changes in cell adhesion and motility. A: Upon direct co-culture with live ADSCs, H358 cells lost homotypic adhesion of epithelial colonies, and became fibrotic individual cells, but not in indirect co-cultures. B-D: To examine changes in cell motility, scratch assays were performed. H358 cells exhibited increased cell motility on live ADSCs, but neither on ECM nor in conditioned media. When H358 cells were sorted from live ADSCs by FACS and plated alone, they immediately formed static epithelial colonies, suggesting that the motility and the morphological changes were reversibly dependent on live cell-cell contact with ADSCs. Scale bar: 50 μm.*

microenvironments has been postulated to play a selective role during cancer evolution, and an intriguing question is whether MSCs or ADSCs can differentiate into specific CAFs tailored to fit individual tumor genetics. For example, H358 cells that have non-metastatic origin, exhibited incomplete or transient EMT-like changes in a previous report: *SMAD3, TWIST* and *SNAI1* were up-regulated, but *CDH1* expression was not repressed (39). When co-cultured with ADSCs or CAFs, A similar biphasic state was again induced (Figure 4). When ADSCs were removed from culture conditions, the EMT-like phenomenon was reversed and cells formed static epithelial colonies. It remains to be addressed whether the EMT-like phenomenon was a reflection of the non-metastatic characteristics specific to H358 cells, or a general phenomenon of stroma- cancer interaction.

In the present study, we showed that ADSCs attached to H358 cells, and triggered EMT-like changes in a similar way to primary CAFs and MSCs *via* NOTCH signaling.

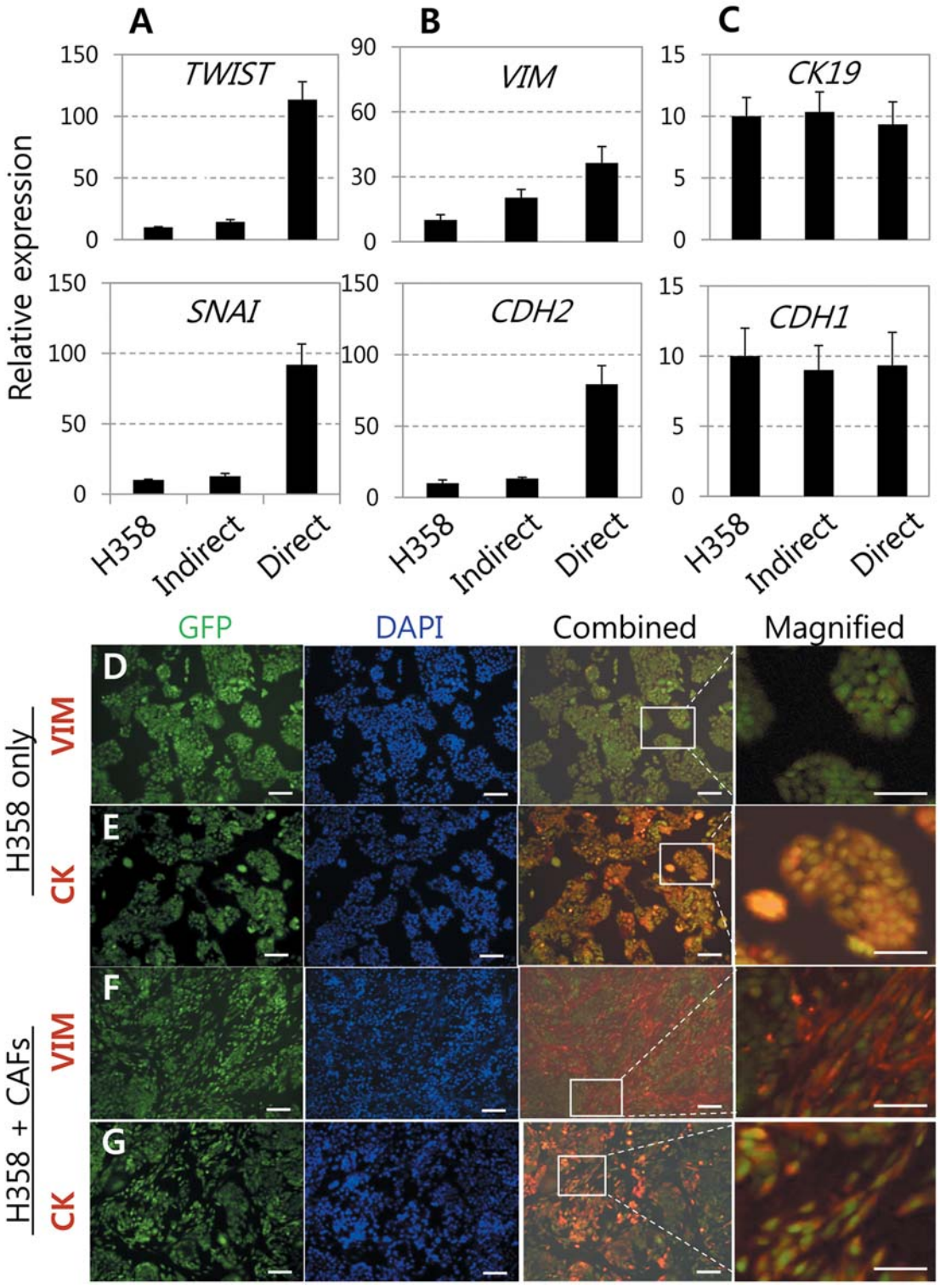

Figure 4. *Epithelial–mesenchymal transition (EMT)-like gene expression in H358 cells. After 48 h of co-culture, H358 cells were sorted from the live adipose-derived mesenchymal stem cells (direct) and gene expression was compared with that in cells maintained in monoculture (H358), or conditioned media/ECM (indirect). TWIST and SNAI1, potent EMT inducers, were significantly up-regulated in direct co-culture (A), as were the downstream mesenchymal markers, VIM and CDH2 (B). Epithelial markers CK19 and CDH1 expression levels showed no significant changes (C), indicating a biphasic state of both epithelial and mesenchymal characteristics. Immunocytochemistry (D-G: unpublished data from 39) showed that H358 cells formed epithelial colonies that express high amount of CK19,and very low amount of VIM (D, E). In co-cultures with CAFs, H358 cells expressed both VIM and CK19 at high levels (F, G). These data suggest that ADSCs and CAFs induced similar EMT-like changes in H358 cells. Scale bar: 50 μm.*

A

Coculture methods	Attachment	EMT
Direct contact	**~ 20 folds**	**Positive**
Conditioned media	Negative	Negative
ECM	**~20 folds**	Negative

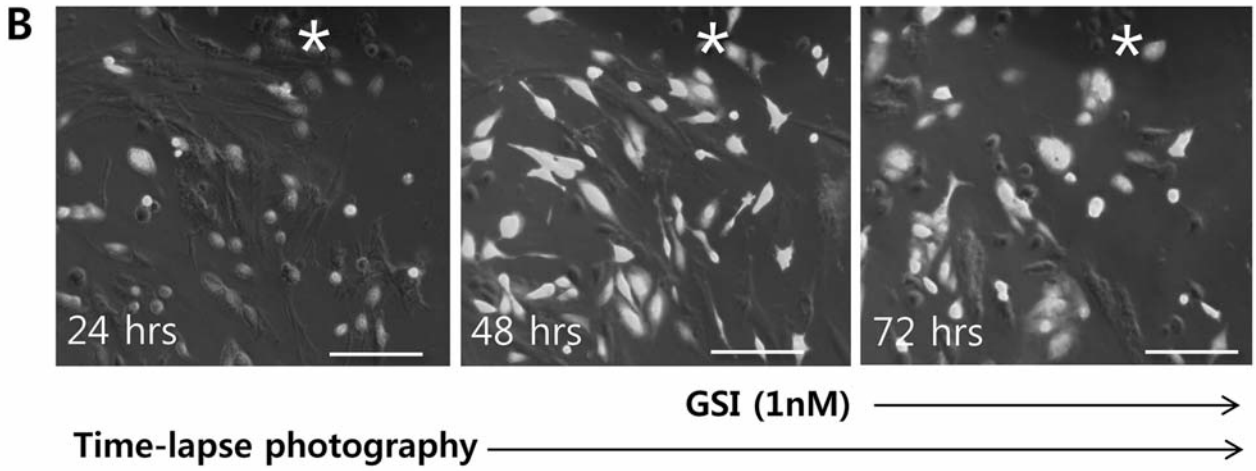

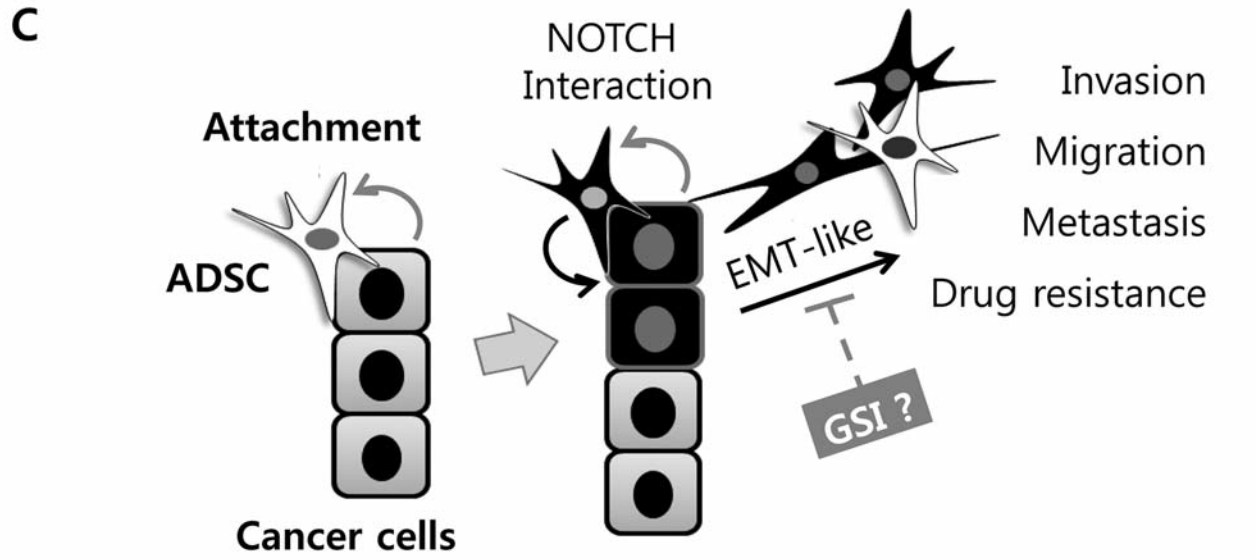

Figure 5. *Identification of NOTCH pathway for epithelial–mesenchymal transition (EMT)-like phenomenon. A: To deduce the candidate signaling pathways underlying the paracrine effects of ADSCs, the effects of direct and indirect co-cultures were compared. Indirect co-cultures with the ECM reproduced the enhanced attachment only, indicating that enhanced attachment is an event independent from the EMT–like phenomenon. On the other hand, conditioned media did not induce EMT–like phenomenon, identifying the direct cell–cell signaling between live ADSCs and H358 cells as the candidate signaling pathway. B: To block the NOTCH pathway, γ–secretase inhibitor was added to the media at 1.0 nM on day 2 of co-culture, and the EMT-like phenomenon was reversed on day 3. A premarked spot (asterisk) shows the same position in the culture dish. C: Summary of the data suggesting that ADSCs attached to H358 lung cancer cells reciprocally interact with each other to induce EMT-like changes that are partially affected by NOTCH inhibitor. Scale bar: 50 μm.*

Acknowledgements

We thank Sung-Whan Moon, Hyung-Min Chung for providing ADSCs, Jhinggook Kim for providing H358 cells, and In Myong Oh, Eung-Sirk Lee, Dae-Soon Son, for scientific advice, and Kwang Jun Lee, and Bo Young Kim for technical assistance. This study was supported by an institution grant from Bundang Jesaeng General Hospital.

References

1 Bremnes RM, Donnem T, Al-Saad S, Al-Shibli K, Andersen S, Sirera R, Camps C, Marinez I and Busaund LT: The role of tumor stroma in cancer progression and prognosis: emphasis on carcinoma-associated fibroblasts and non-small cell lung cancer. J Thorac Oncol *6*: 209-217, 2011.

2 Kalluri R and Zeisberg M: Fibroblasts in cancer. Nat Rev Cancer *6*: 392-401, 2006.

3 Greaves M and Maley CC: Clonal evolution in cancer. Nature *481*: 306-313, 2012.

4 Psaila B and Lyden D: The metastatic niche: Adapting the foreign soil. Nat Rev Cancer *4*: 285-293, 2009.

5 Langley RR and Fidler IJ: The seed and soil hypothesis revisited, the role of tumor- stroma interactions in metastasis to different organs. Int J Cancer *128*: 2527-2535, 2011.

6 Yoneda T and Hiraga T: Crosstalk between cancer cells and bone microenvironment in bone metastasis. Biochem Biophys Res Commun *328*: 679-687, 2005.

7 Tobita M, Orbay H and Mizuno H: Adipose-derived stem cells: Current findings and future perspectives. Discov Med *11*: 160-170, 2011.

8 Mizuno H, Tobit M and Uysal AC: Concise review: Adipose-derived stem cells as a novel tool for future regenerative medicine. Stem Cells *30*: 804-810, 2012.

9 Klopp AH, Zhang Y, Solley T, Amaya-Manzanares F, Marini F, Andreeff M, Debeb B, Woodward W, Schmandt R, Broaddus R, Lu K and Kolonin MG: Omental adipose tissue-derived stromal cells promote vascularization and growth of endometrial tumors. Clin Cancer Res *18*: 771-782, 2012.

10 Zhao BC, Zhao B, Han JG, Ma HC and Wang ZJ: Adipose-derived stem cells promote gastric cancer cell growth, migration and invasion through SDF-1/CXCR4 axis. Hepatogastroenterology *57*: 1382-1389, 2010.

11 Zimmerlin L, Donnenberg AD, Rubin JP, Basse P, Landreneau RJ and Donnenberg VS: Regenerative therapy and cancer: *In vitro* and *in vivo* studies of the interaction between adipose-derived stem cells and breast cancer cells from clinical isolates. Tissue Eng Part A *17*: 93-106, 2011.

12 Bergfeld SA and DeClerck YA: Bone marrow-derived mesenchymal stem cells and the tumor microenvironment. Cancer Metastasis Rev *29*: 249-261, 2011.

13 Kabashima-Niibe A, Higuchi H, Takaishi H, Masugi Y, Matsuzaki Y, Mabuchi Y, Funakoshi S, Adachi M, Hamamoto Y, Kawachi S, Aiura K, Kitagawa Y, Sakamoto M and Hibi T: Mesenchymal stem cells regulate epithelial–mesenchymal transition and tumor progression of pancreatic cancer cells. Cancer Sci *104*: 157-164, 2013.

14 Mizuno H: Adipose-derived stem and stromal cells for cell-based therapy: current status of preclinical studies and clinical trials. Curr Opin Mol Ther *12*: 442-449, 2010.

15 Straussman R, Morikaw T, Shee K, Barzily-Rokni M, Qian ZR, Du J, Davis A, Mongare MM, Gould J, Frederick DT, Cooper ZA, Chapman PB, Solit DB, Ribas A, Lo RS, Flaherty KT, Ogino S, Wargo JA and Golub TR: Tumor microenvironment elicits innate resistance to RAF inhibitors through HGF secretion. Nature *487*: 500-504, 2012.

16 Orimo A, Gupta PB, Sgroi DC, Arenzana-Seisdedos F, Delaunay T, Naeem R, Carey VJ, Richardson AL and Weinberg RA: Stromal fibroblasts present in invasive human breast carcinomas promote tumor growth and angiogenesis through elevated SDF-1/CXCL12 secretion. Cell *121*: 335-348, 2005.

17 Wang W, Li Q and Yamada T: Crosstalk to stromal fibroblasts induces resistance of lung cancer to epidermal growth factor receptor tyrosine kinase inhibitors. Clin Cancer Res *15*: 6630-6638, 2009.

18 Mink SR, Vashistha S and Zhang W: Cancer-associated fibroblasts derived from EGFR-TKI-resistant tumors reverse EGFR pathway inhibition by EGFR-TKIs. Mol Cancer Res *6*: 809-820, 2010.

19 Miki Y, Ono K and Hata S: The advantages of co-culture over mono cell culture in simulating *in vivo* environment. J. Steroid Biochem Mol Biol *131*: 68-75, 2012.

20 Fiaschi T, Giannoni E, Taddei ML, Cirri P, Marini A, Pintus G, Nativi C, Richichi B, Scozzafava A, Carta F, Torre E, Supuran CT and Chiarugi P: Carbonic anhydrase IX from cancer-associated fibroblasts drives epithelial–mesenchymal transition in prostate carcinoma cells. Cell Cycle *12*: 1791-1801, 2013.

21 Soon PS, Kim E, Pon CK, Gill AJ, Moore K, Spillane AJ, Benn DE and Baster RC: Breast cancer-associated fibroblasts induce epithelial-to-mesenchymal transition in breast cancer cells. Endocr Relat Cancer *20*: 1-12, 2013.

22 Bhattacharya SD, Mi Z, Talbot LJ, Guo H and Kuo PC: Human mesenchymal stem cell and epithelial hepatic carcinoma cell lines in admixture: Concurrent stimulation of cancer-associated fibroblasts and epithelial–to–mesenchymal transition markers. Surgery *152*: 449-454, 2012.

23 Gao MQ, Kim BG, Kang S, Choi YP, Park H, Kang KS and Cho NH: Stromal fibroblasts from the interface zone of human breast carcinomas induce an epithelial–mesenchymal transition-like state in breast cancer cells *in vitro*. J Cell Sci *123*: 3507-3514, 2010.

24 Soltermann A, Tischler V, Arbogast S, Braun J, Probst-Hensch N, Weder W, Moch H and Kristiansen G: Prognostic significance of epithelial–mesenchymal and mesenchymal- epithelial transition protein expression in non-small cell lung cancer. Clin Cancer Res *14*: 7430-7437, 2008.

25 Hu M, Peluffo G, Chen H, Gelman R, Schnitt S and Polyak K: Role of COX-2 in epithelial–stromal cell interactions and progression of ductal carcinoma *in situ* of the breast. Proc Natl Acad Sci USA *106*: 3372-3377, 2009.

26 Amatangelo MD, Goodyear S, Varma D and Stearns ME: c-MYC expression and MEK1-induced ERK2 nuclear localization are required for TGF-beta induced epithelial–mesenchymal transition and invasion in prostate cancer. Carcinogenesis *33*: 1965-1975, 2012.

27 DiMeo TA, Anderson K, Phadke PC, Fan C, Perou CM, Naber S and Kuperwasser C: A novel lung metastasis signature links Wnt signaling with cancer cell self-renewal and epithelial–mesenchymal transition in basal-like breast cancer. Cancer Res *69*: 5364-5373, 2009.

28 Yilmaz M and Christofori G: EMT, the cytoskeleton, and cancer cell invasion. Cancer Metastasis Rev *28*: 15-33, 2009.
29 Suzuki H, Masuda N, Shimura T, Araki K, Kobayashi T, Tsutsumi S, Asao T and Kuwano H: Nuclear β-catenin expression at the invasive front and in the vessels predicts liver metastasis in colorectal carcinoma. Anticancer Res *28*: 1821-1830, 2008.
30 Hlubek F., Brabletz T, Budczies J, Pfeiffer S, Jung A and Kirchner T: Heterogeneous expression of Wnt/β-catenin target genes within colorectal cancer. Int J Cancer *121*: 1941-1948, 2007.
31 Moustakas A and Heldin CH: Signaling networks guiding epithelial–mesenchymal transitions during embryogenesis and cancer progression. Cancer Sci *98*: 1512-1520, 2007.
32 Thiery JP, Acloque H, Huang RY and Nieto MA: Epithelial–mesenchymal transitions in development and disease. Cell *139*: 871-890, 2009.
33 Kim YC, Clark RJ, Ranheim EA and Alexander CM: Wnt1 expression induces short-range and long-range cell recruitments that modify mammary tumor development and are not induced by a cell-autonomous β-catenin effector. Cancer Res *68*: 10145–10153, 2008.
34 Xie M, Zhang L, He CS, Xu F, Liu JL, Hu AH, Zhao LP and Tian Y: Activation of Notch-1 enhances epithelial–mesenchymal transition in gefitinib-acquired resistant lung cancer cells. J Cell Biochem *113*: 1501-1513, 2012.
35 Vergara D, Merlot B, Lucot JP, Collinet P, Vinatire D, Fournier I and Salzet M: Epithelial– mesenchymal transition in ovarian cancer. Cancer Lett *291*: 59-66, 2010.
36 Zhang K, Corsa CA, Ponik SM, Prior JL, Piwnica-Worms D, Eliceiri KW, Keely PJ and Longmore GD: The collagen receptor discoidin domain receptor 2 stabilizes SNAI1 to facilitate breast cancer metastasis. Nat Cell Biol *15*: 677-687, 2010.
37 Das TP, Suman S and Damodaran C: Reactive oxygen species generation inhibits epithelial–mesenchymal transition and promotes growth arrest in prostate cancer cells. Mol Carcinog doi: 10.1002/mc.22014. Epub ahead of print, 2013.
38 Nyhan KC, Faherty N, Murray G, Cooey LB, Godson C, Crean JK and Brazil DP: JAGGED/NOTCH signalling is required for a subset of TGFβ1 responses in human kidney epithelial cells. Biochim Biophys Acta *1803*: 1386-1395, 2010.
39 Kim SH, Choe C, Shin YS, Jeon MJ, Choi SJ, Lee J, Bae GY, Cha HJ and Kim J: Human lung cancer-associated fibroblasts enhance motility of non-small cell lung cancer cells in co-culture. Anticancer Res *33*: 2001-2009, 2013.
40 Katoh M and Katoh M: Integrative genomic analyses of ZEB2: Transcriptional regulation of ZEB2 based on SMADs, ETS1, HIF1α, POU/OCT, and NF-κB. Int J Oncol *34*: 1737-1742, 2009.
41 Fiaschi T, Marini A, Giannoni E, Taddei ML, Gandellini P, De Donatis A, Lanciotti M, Sermi S, Cirri P and Chiarugi P: Reciprocal metabolic reprogramming through lactate shuttle coordinately influences tumor- stroma interplay. Cancer Res *72*: 5130-5140, 2012.

Received July 16, 2013
Revised September 10, 2013
Accepted September 11, 2013